

A DYNAMIC MODEL OF THE SLATER K.D.P. FERROELECTRIC

By R. D. IRVINE*

[Manuscript received April 17, 1970]

Abstract

Several dynamical models of the Slater K.D.P. model of a ferroelectric are studied and, following Glauber, master equations are derived for the time development of these models. A computer simulation of the models is used to study the solutions to these equations, and to compare the equilibrium results with Lieb's exact solution of the equilibrium case. Excellent agreement is obtained in one case.

I. INTRODUCTION

Recently, Lieb (1967*a*, 1967*b*, 1967*c*, 1967*d*) obtained an exact solution to the 2D Slater K.D.P. ferroelectric problem, along with the related ice and Rys F model problems. These solutions, together with the classic Ising model solution of Onsager (1944), provide very interesting information on some reasonably realistic, if simplified, models which undergo order-disorder phase transitions. However, the exact solutions describe only the equilibrium behaviour, and some effort has been put into obtaining information on the non-equilibrium behaviour of these systems. Glauber (1963), Kawasaki and Yamada (1967), and others have studied the time-dependent Ising model by analytic methods, while Ogita *et al.* (1969) report on a computer simulation of an order-disorder transition. While Ogita *et al.* apply their results to K.D.P., Frohlich and Fisher (quoted from Ogita *et al.* 1969) have pointed out correctly that although the results apply to the Ising model, the K.D.P. model cannot be reduced to an Ising-type model, because of the so-called "ice rules" of hydrogen bonding.

Onsager and Dupuis (1960, 1962) and Onsager and Runnels (personal communication) have discussed a model for the dynamical behaviour of the hydrogen-bonded models, involving the diffusion of defects. In the present paper, results are reported of a computer simulation of this model and of an approximation of this introduced by Onsager and Runnels (personal communication). The exact Onsager-Slater model shows the correct transition point, predicted in Lieb's solution, and confirms the existence of an anomalously slow relaxation phenomenon near the transition point, similar to that in the results of Ogita *et al.* (1969) for the Ising model. However, in other ways the transition differs markedly from the Ising transition; in particular there is no simple nearest-neighbour correlation or "clustering" for the Slater model as there was for the Ising model.

The behaviour in an electric field is quite different, the Slater model having a metastable state at low temperatures and low fields. The Onsager-Runnels approximation is unsatisfactory for K.D.P. at low temperatures, and does not show a transition to an ordered state at any temperature.

* Department of Mathematical Physics, University of Adelaide, P.O. Box 498D, Adelaide, S.A. 5001.

II. SLATER K.D.P. MODEL

The Slater K.D.P. model was proposed by Slater (1941) to account for the ferroelectric behaviour of potassium dihydrogen phosphate (K.D.P.). This compound consists of phosphate radicals hydrogen-bonded to each other in a diamond-like lattice. Thus each phosphate group is surrounded by four hydrogen bonds. In common with the other hydrogen-bonded models for ice and the Rys F antiferroelectric, the proton forming the hydrogen bond is considered to be near one end or other of the bond. Further, the "ice rule" states that ionization of a phosphate group is very unlikely, and therefore each phosphate group has exactly two protons near it. This reduces the possible arrangements around a lattice point (phosphate group) to six. Slater proposed that if the resultant dipole was lined up parallel or antiparallel to a particular axis, the c axis, it would have a lower energy than if it were perpendicular to that axis. The 2D model is produced by projecting the 3D lattice onto a plane perpendicular to the c axis. This produces a square lattice with vertical and horizontal bonds connecting all vertices. The allowed vertex configurations and their energies are shown in Figure 1.





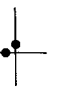

Vertex No.	1	2	3	4	5	6
						
Energy	0	$+\epsilon$	$+\epsilon$	$+\epsilon$	$+\epsilon$	0
Polarization	$+D$	$+D$	0	0	$-D$	$-D$

Fig. 1.—Slater K.D.P. lattice configurations.

Slater (1941) correctly predicted a first-order (latent heat) transition at the critical temperature $T_c = \epsilon/k \ln 2$, where ϵ is the vertex energy in Figure 1 and k is Boltzmann's constant. Lieb (1967*a*, 1967*b*, 1967*c*, 1967*d*) confirmed this in his exact solution, as well as giving the specific heat and polarizability. The model is interesting in that, below the critical point, the lattice is completely polarized. The lattice remains in one of the two ground states until the critical point, where there is a latent heat $\frac{1}{2}N\epsilon$, N being the number of lattice sites. The polarization as a function of electric field below T_c is a step function, with complete polarization in the direction of the field for arbitrary small fields.

III. ONSAGER-SLATER DYNAMICAL MODEL

It should be noted that the Slater model by itself provides no means of transition from one state of the lattice to any other. Any "flipping" of a lattice point from one vertex configuration to a different one will violate one or other of the assumptions of hydrogen bonding: (1) that there is exactly one proton per bond, and (2) that there are exactly two protons near each vertex. In order to allow transitions to occur, relaxations must be made on these restrictions. Much research has gone into the dynamical behaviour of ice, which has very similar hydrogen bonding, and the

mechanisms devised by Bjerrum (1951) and discussed by Onsager and Dupuis (1960, 1962) and Onsager and Runnels (personal communication) have proved very successful in that case.

The mechanisms consist of allowing a very small number of defects to occur in the lattice. The first type of defect, the Bjerrum defect, consists of a bond with two, or no, protons. Each bond has two associated vertices and either of these can rotate (in the three-dimensional sense) to correct the defective bond, at the same time moving the defect to another bond attached to the same vertex. Thus the Bjerrum defect "migrates" through the lattice, leaving a trail of "flipped" vertices behind, each vertex still obeying the rules of hydrogen bonding. This Bjerrum defect migration is illustrated in Figure 2(a).

The second type of defect breaks rule (2) of hydrogen bonding: there are three, or one, protons near a vertex. Thus the vertex is "ionized" in the sense that it contains one excess or one too few protons. One of the protons on the bonds surrounding a vertex may "flip" to correct the number of protons on that vertex, and the defect is moved to a neighbouring vertex. The "ion" defect thus also migrates through the lattice. This is illustrated in Figure 2(b).

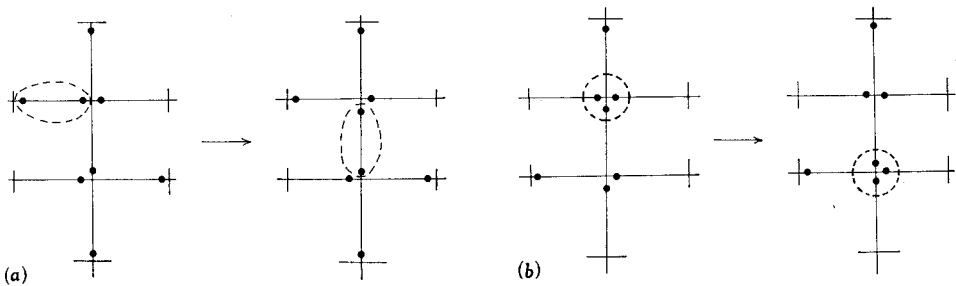


Fig. 2.—Illustrating the migration of (a) a Bjerrum defect and (b) an ionic defect.

Both types of defect, of course, must exist in pairs of positive (two protons per bond or three per vertex) and negative (no protons per bond, or one per vertex) defects, and the present theory allows pair creation and annihilation. The probability of creation is kept sufficiently small to allow all other defect-defect interaction to be ignored.

For convenience in the analytical treatment of this model, in the case of electrical relaxation in ice Onsager and Runnels (personal communication) have used an approximation to Bjerrum migration which removes the dependence of the migration of the Bjerrum defects on the actual neighbouring bond configurations by replacing the actual transition probabilities with a "mean" value of the transition probability. This has the effect of allowing "forbidden" transitions to occur, and the defect migrates leaving a trail of defective bonds in its wake. This approximation has given some useful results in the ice problem, which has no critical point, and it is of interest to see whether the approximation preserves the characteristics of the transition in models with order-disorder transitions, since it is very much easier to handle analytically.

IV. FORMULATION OF THE TIME-DEPENDENT MODEL

Following Glauber (1963), we now attempt to set up a master equation which will describe the time-dependent development of the models described. The Slater model, as originally formulated, has no time development, so the first model considered will be the Onsager-Slater version.

There are two ways of transforming the lattice into a set of spins. The first represents each lattice point by a spin variable S_{ij} which can take any of six values, corresponding to the six different vertex configurations. This representation is suitable for considering Bjerrum defects, since this type of defect is essentially a defective bond while all vertices are correct. The alternate, and far simpler, representation transforms the lattice into a set of spins σ_{ij}^z with each spin representing a bond and taking only two values (± 1). This is suitable for considering ion defects, which are vertex defects, the bonds being correct. In order to avoid the complexity of a six-valued spin variable, we will consider the latter representation.

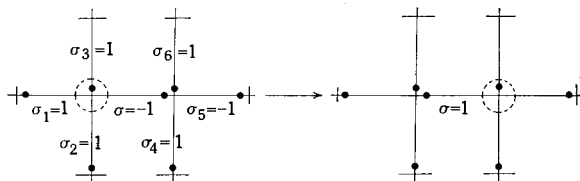


Fig. 3.—Typical ionic defect transition.

The K.D.P. model in two dimensions is represented as a set of spins σ_{ij}^α ($i, j = 1, 1, \dots, M, N$; $\alpha = 0, 1$) where each spin σ_{ij}^α represents a bond on the $M \times N$ square lattice leading from the point (i, j) to the point $(i + \alpha, j + 1 - \alpha)$, with $\alpha = 0$ for vertical bonds and 1 for horizontal bonds.

The ground state of the lattice is then represented by a set of spins $\{\sigma_{ij}^\alpha\}$ all of which are equal to $+1$. A bond that has “flipped” has $\sigma_{ij}^\alpha = -1$. The “ice condition” becomes

$$\sigma_{ij}^0 + \sigma_{ij}^1 - \sigma_{i-1,j}^1 - \sigma_{i,j-1}^0 = 0 \quad \text{for all } i, j \quad (1)$$

Using the cyclic boundary conditions

$$\sigma_{M+1,j}^\alpha = \sigma_{1j}^\alpha, \quad \sigma_{i,N+1}^\alpha = \sigma_{i1}^\alpha, \quad (2)$$

and writing the probability of a particular spin configuration $\sigma_{11}^0, \dots, \sigma_{MN}^0$; $\sigma_{11}^1, \dots, \sigma_{MN}^1$ at time t as

$$P(\sigma_{11}^0, \dots, \sigma_{MN}^1, t),$$

we can write, as in Glauber (1963),

$$\begin{aligned} \frac{d}{dt} \left(P(\sigma_{11}^0, \dots, \sigma_{MN}^1, t) \right) = & \left(\sum_{ij\alpha} \omega_{ij}^\alpha (-\sigma_{ij}^\alpha) P(\sigma_{11}^0, \dots, -\sigma_{ij}^\alpha, \dots, \sigma_{MN}^1, t) \right) \\ & - \left(\sum_{ij\alpha} \omega_{ij}^\alpha (\sigma_{ij}^\alpha) P(\sigma_{11}^0, \dots, \sigma_{MN}^1, t) \right), \end{aligned} \quad (3)$$

where $\omega_{ij}^\alpha(\sigma)$ is the probability of a flip from σ to $-\sigma$ at the site (ij) .

Using the conventional K.D.P. lattice energies and putting $\gamma = \tanh(\epsilon/2kT)$, we can write down the transition probability $\omega_{ij}^\alpha(\sigma)$ for any given arrangement of the neighbouring spins, for which we introduce the notation

$$\begin{aligned}\sigma_1 &= \sigma_{i-\alpha, j-1+\alpha}, & \sigma_2 &= \sigma_{i-1+\alpha, j-\alpha}, & \sigma_3 &= \sigma_{ij}^{1-\alpha}, \\ \sigma_4 &= \sigma_{i-1+2\alpha, j+1-2\alpha}, & \sigma_5 &= \sigma_{i+\alpha, j+1-\alpha}, & \sigma_6 &= \sigma_{i+\alpha, j+1-\alpha}^{1-\alpha}.\end{aligned}$$

For example, in the case illustrated in Figure 3, we have $\alpha = 1$, $\sigma = -1$, $\sigma_1 = \sigma_2 = \sigma_3 = \sigma_4 = \sigma_6 = 1$, and $\sigma_5 = -1$. There is a negative defect at the vertex (ij) . The defect will be corrected by a transition at the bond $(\frac{1}{ij})$, with a transition energy of $-\epsilon$. Hence in this case we can write the transition probability

$$\omega_{ij}^\alpha = \kappa \exp(\epsilon/kT) / \{1 + \exp(\epsilon/kT)\} = \frac{1}{2} \kappa (1 + \gamma),$$

where κ is an arbitrary rate term. Hence the contribution of this configuration of neighbouring spins is given by

$$(\kappa/2^8)(\sigma_1+1)(\sigma_2+1)(\sigma_3+1)(\sigma_4+1)(\sigma_5-1)(\sigma_6+1)(\sigma-1)(1+\gamma).$$

By calculating these terms for all possible neighbouring configurations and summing, we can write $\omega_{ij}^\alpha(\sigma)$ in the form

$$\omega_{ij}^\alpha(\sigma) = (\kappa/2^8)(B+2C\gamma\sigma), \quad (4)$$

where B and C are sixth-order polynomials in the six neighbouring spins $\sigma_1, \dots, \sigma_6$:

$$\begin{aligned}B &= \{18-6(\sigma_1\sigma_2+\sigma_5\sigma_6)-2(\sigma_3\sigma_4+\sigma_1\sigma_5+\sigma_1\sigma_6+\sigma_2\sigma_5+\sigma_2\sigma_6) \\ &\quad +2(\sigma_1\sigma_4+\sigma_2\sigma_4+\sigma_3\sigma_5+\sigma_3\sigma_6)+6(\sigma_1\sigma_3+\sigma_2\sigma_3+\sigma_4\sigma_5+\sigma_4\sigma_6) \\ &\quad +6(\sigma_1\sigma_2\sigma_3\sigma_4+\sigma_3\sigma_4\sigma_5\sigma_6)+2(\sigma_1\sigma_2\sigma_5\sigma_6+\sigma_1\sigma_3\sigma_4\sigma_5+\sigma_1\sigma_3\sigma_4\sigma_6 \\ &\quad +\sigma_2\sigma_3\sigma_4\sigma_5+\sigma_2\sigma_3\sigma_4\sigma_6)-2(\sigma_1\sigma_2\sigma_4\sigma_5+\sigma_1\sigma_2\sigma_4\sigma_6+\sigma_1\sigma_3\sigma_5\sigma_6+\sigma_2\sigma_3\sigma_5\sigma_6) \\ &\quad -6(\sigma_1\sigma_2\sigma_3\sigma_5+\sigma_1\sigma_2\sigma_3\sigma_6+\sigma_1\sigma_4\sigma_5\sigma_6+\sigma_2\sigma_4\sigma_5\sigma_6)-18\sigma_1\sigma_2\sigma_3\sigma_4\sigma_5\sigma_6\}, \quad (5a)\end{aligned}$$

$$\begin{aligned}C &= \{-6-4(\sigma_1+\sigma_2+\sigma_5+\sigma_6)-8(\sigma_3+\sigma_4)+10(\sigma_1\sigma_2+\sigma_5\sigma_6)+6\sigma_3\sigma_4 \\ &\quad +2(\sigma_1\sigma_3+\sigma_2\sigma_3+\sigma_4\sigma_5+\sigma_4\sigma_6)-2(\sigma_1\sigma_4+\sigma_1\sigma_5+\sigma_1\sigma_6+\sigma_2\sigma_4+\sigma_2\sigma_5 \\ &\quad +\sigma_2\sigma_6+\sigma_3\sigma_5+\sigma_3\sigma_6)+4(\sigma_1\sigma_2\sigma_5+\sigma_1\sigma_2\sigma_6+\sigma_1\sigma_3\sigma_6+\sigma_2\sigma_5\sigma_6) \\ &\quad -4(\sigma_1\sigma_3\sigma_4+\sigma_2\sigma_3\sigma_4+\sigma_3\sigma_4\sigma_5+\sigma_3\sigma_4\sigma_6)-10(\sigma_1\sigma_2\sigma_3\sigma_4+\sigma_3\sigma_4\sigma_5\sigma_6) \\ &\quad -6\sigma_1\sigma_2\sigma_5\sigma_6-2(\sigma_1\sigma_2\sigma_3\sigma_5+\sigma_1\sigma_2\sigma_3\sigma_6+\sigma_1\sigma_4\sigma_5\sigma_6+\sigma_2\sigma_4\sigma_5\sigma_6) \\ &\quad +2(\sigma_1\sigma_2\sigma_4\sigma_5+\sigma_1\sigma_2\sigma_4\sigma_6+\sigma_1\sigma_3\sigma_4\sigma_5+\sigma_1\sigma_3\sigma_4\sigma_6+\sigma_1\sigma_4\sigma_5\sigma_6+\sigma_2\sigma_3\sigma_4\sigma_5 \\ &\quad +\sigma_2\sigma_3\sigma_4\sigma_6+\sigma_2\sigma_3\sigma_5\sigma_6)+4(\sigma_1\sigma_2\sigma_3\sigma_4\sigma_5+\sigma_1\sigma_2\sigma_3\sigma_4\sigma_6+\sigma_1\sigma_3\sigma_4\sigma_5\sigma_6 \\ &\quad +\sigma_2\sigma_3\sigma_4\sigma_5\sigma_6)+8(\sigma_1\sigma_2\sigma_3\sigma_5\sigma_6+\sigma_1\sigma_2\sigma_4\sigma_5\sigma_6)+6\sigma_1\sigma_2\sigma_3\sigma_4\sigma_5\sigma_6\}. \quad (5b)\end{aligned}$$

The form of this dependence on nearest neighbours is far from the simple form of the Ising model, and does not easily lend itself to an approach such as Glauber's, but it does have a similarly simple interpretation. The function B is zero for forbidden

transitions (i.e. bonds between normal vertices) and unity for allowed defect migration (i.e. bonds on a defective vertex). The function C is again zero for all forbidden transitions, and for allowed transitions it takes values that produce the appropriate Maxwell-Boltzmann factors. Thus for allowed transitions, corresponding to lattice points with a defect, equation (4) reduces to a form similar to that of Glauber.

For simplicity, equation (4) does not include probabilities for creation and annihilation of defects, but these can be included with no difficulty by means of a third term,

$$\omega_{ij}^z(\sigma) = (\kappa/2^8)(B+2C\gamma\sigma+D\lambda), \quad (4a)$$

where λ is the appropriate Maxwell-Boltzmann factor for the (large) pair creation energy and D is a similar polynomial to B and C , taking nonzero values for forbidden transitions (non-defective, or doubly defective bonds).

We will try to write the migration of Bjerrum faults in a similar form. We now have a six-valued spin S_{ij} (representing the six different vertex configurations) but only four neighbours, $S_{i-1,j}$, $S_{i,j-1}$, $S_{i+1,j}$, and $S_{i,j+1}$. The master equation becomes

$$\begin{aligned} \frac{d}{dt} \left(P(S_{11}, \dots, S_{MN}, t) \right) = & \left(\sum_{i,j} \sum_{S'_{i,j}} \Omega_{ij}(S'_{ij}, S_{ij}) P(S_{11}, \dots, S'_{ij}, \dots, S_{MN}, t) \right) \\ & - \left(\sum_{ij} \sum_{S'_{ij}} \Omega_{ij}(S_{ij}, S'_{ij}) \right) P(S_{11}, \dots, S_{MN}, t), \end{aligned} \quad (6)$$

where $\Omega_{ij}(S', S)$ is the probability of a flip from S' to S at site (i, j) . Thus, $\Omega_{ij}(S', S)$ is a 6×6 matrix.

Each of the 36 terms of $\Omega_{ij}(S', S)$ is a function of the four neighbours $S_{i-1,j}$, $S_{i,j-1}$, $S_{i+1,j}$, $S_{i,j+1}$, and thus each term of Ω is a $6 \times 6 \times 6 \times 6$ "matrix". Moreover, we no longer have the simplicity of the two-valued spin notation, which allowed us to use the simple δ functions $\frac{1}{2}(1+\sigma)$ and $\frac{1}{2}(1-\sigma)$. Hence, although the value of Ω is quite obvious in each case, to write out all 6^6 terms would be both tedious and meaningless.

However, we can indicate that equations (3) and (6) are essentially equivalent. Obviously, for any lattice with no defects, represented by the bond notation $\{\sigma_{ij}^z\}$, we can construct an equivalent lattice, using the vertex notation $\{S_{ij}\}$, which is equivalent at each lattice site in an obvious way. Similarly, for low defect concentrations, for any lattice represented in bond notation, we can construct an "equivalent" lattice in the vertex notation, in which the equivalence relation maps non-defective lattice sites in the obvious manner, and maps ionic defects to Bjerrum defects where the lattice is defective. This equivalence relation, at least for low enough defect concentrations, maps the possible sets $\{\sigma_{ij}^z\}$ onto the possible sets $\{S_{ij}\}$. To show the equivalence of equations (3) and (6), we need only show that the ionic and Bjerrum defects traverse the "same" path through their respective lattices and leave the lattices in the "same" final state. This is assured by the way we constructed the transition probabilities $\omega_{ij}^z(\sigma)$ and $\Omega_{ij}(S, S')$, depending only on the state of the lattice before and after the transition and not on any defect properties, and by choosing the correct mapping from ionic defects to Bjerrum defects.

This "equivalence" emphasizes the point that the Bjerrum and Onsager theories of defect migration provide a catalyst for transitions in the Slater K.D.P. model, but in no way influence the critical point or equilibrium behaviour of the model.

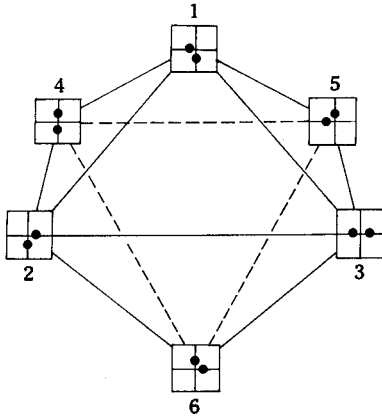


Fig. 4.—Allowed transitions in the Onsager–Runnels approximation. Bjerrum defect migrations produce transitions between states joined by an edge of the octahedral diagram.

The approximation introduced by Onsager and Runnels (personal communication) removes the dependence of Ω on the neighbouring spins. If we let $S_{ij} = 1, 2, \dots, 6$, and associate vertex configurations as numbered in Figure 1, then it can be seen that, if we ignore neighbouring spins, a vertex in state S can rotate to any of four different configurations (Fig. 4). After taking into account the energies of the various configurations, we can write the transition matrix as

$$\Omega = \frac{1}{4} \begin{pmatrix} 0 & 1 & 1 & 1 & 1 & 0 \\ 1+\gamma & 0 & 1-\gamma & 1-\gamma & 0 & 1+\gamma \\ 1+\gamma & 1-\gamma & 0 & 0 & 1-\gamma & 1+\gamma \\ 1+\gamma & 1-\gamma & 0 & 0 & 1-\gamma & 1+\gamma \\ 1+\gamma & 0 & 1-\gamma & 1-\gamma & 0 & 1+\gamma \\ 0 & 1 & 1 & 1 & 1 & 0 \end{pmatrix}.$$

However, to write the transition probabilities in this form amounts to an almost total relaxation of the first rule of hydrogen bonding. No account is taken of the configuration of the neighbouring vertices, and hence the migration of the defect proceeds leaving in its wake a trail of mismatched bonds, which constitute a host of new defects. This approximation is therefore expected to have an appreciable effect on the equilibrium of the system, since the defects can no longer be considered a negligible part of the lattice, and do not act merely as a catalyst.

Another approximation that springs to mind would be to introduce a similar relaxation of the second hydrogen-bonding rule, by considering a lattice of bonds with no constraints at the vertices. Such a system no longer bears any resemblance to the Slater K.D.P. model, since, as any lattice configuration is allowed, the six vertex energies prescribed by Slater can no longer be used to determine the state of the system. There are a further 10 possible configurations for which no value of energy is specified.

Ogita *et al.* (1969) attempted to compensate for this by introducing bond interaction with nearest and next-nearest neighbours, but this is an Ising-type model,

with very different characteristics. In Ising models, a short-range force "encourages" neighbouring spins to line up, and hence spread ordering through the lattice. This is not so in the hydrogen-bonded lattice models. Here the flipping of one bond requires the flipping of an entire chain of bonds, thus achieving long-range results from a short-range force.

In fact, the nature of the K.D.P. transition is not so much an order-disorder transition as a ground state to excited state transition. The lowest energy has just two states, $\sigma_{ij}^z = 1$ for all i, j, α and $\sigma_{ij}^z = -1$ for all i, j, α . The next lowest energy is that of those states with the smallest possible chain of flipped bonds, which, in an $N \times N$ lattice, is of length N and hence energy $N\epsilon$. For large N , this energy gap is large compared with the individual energy associated with spin alignment.

V. COMPUTER SIMULATION

The method used was essentially similar to that employed by Ogita *et al.* (1969). Temperature and external field are read in as data. The lattice is set up as an array of spins in the computer, initially in a completely ordered state. A spin is chosen at random and a pair of defects is created at this point. Then, at each cycle of the program, the computer randomly decides to create another defect pair or to displace an existing defect from its present site to an adjacent site. Occasionally, a defect will meet an opposite defect and the two are annihilated. The number of defects present in the lattice at the same time thus reaches an equilibrium which is controlled by a probability parameter, preset to ensure that the number is small. If the computer decides to displace a defect, the defect is chosen at random from a list of those in the lattice, and the direction in which the defect is to migrate is also selected at random, with a probability weighting depending on the state of the adjacent spins. After each cycle, the new state of the lattice is stored along with a list of all defects and their positions.

After a large number of cycles have elapsed, the energy, polarization, and pattern of the bond configuration are output. This is repeated until the system attains equilibrium. The lattice size was usually chosen to be 100×100 with periodic boundary conditions, although a few runs with a 128×128 lattice were carried out. The number of program cycles required to bring the system to equilibrium varied from less than 5×10^5 for temperatures far from the critical point to up to 2×10^7 for temperatures very near the critical point. For these long runs, the system had still not reached a steady final energy and had very large fluctuations, so it was not easy to determine if "equilibrium" had been reached. The computer used was a CDC 6400 at the University of Adelaide Computing Centre.

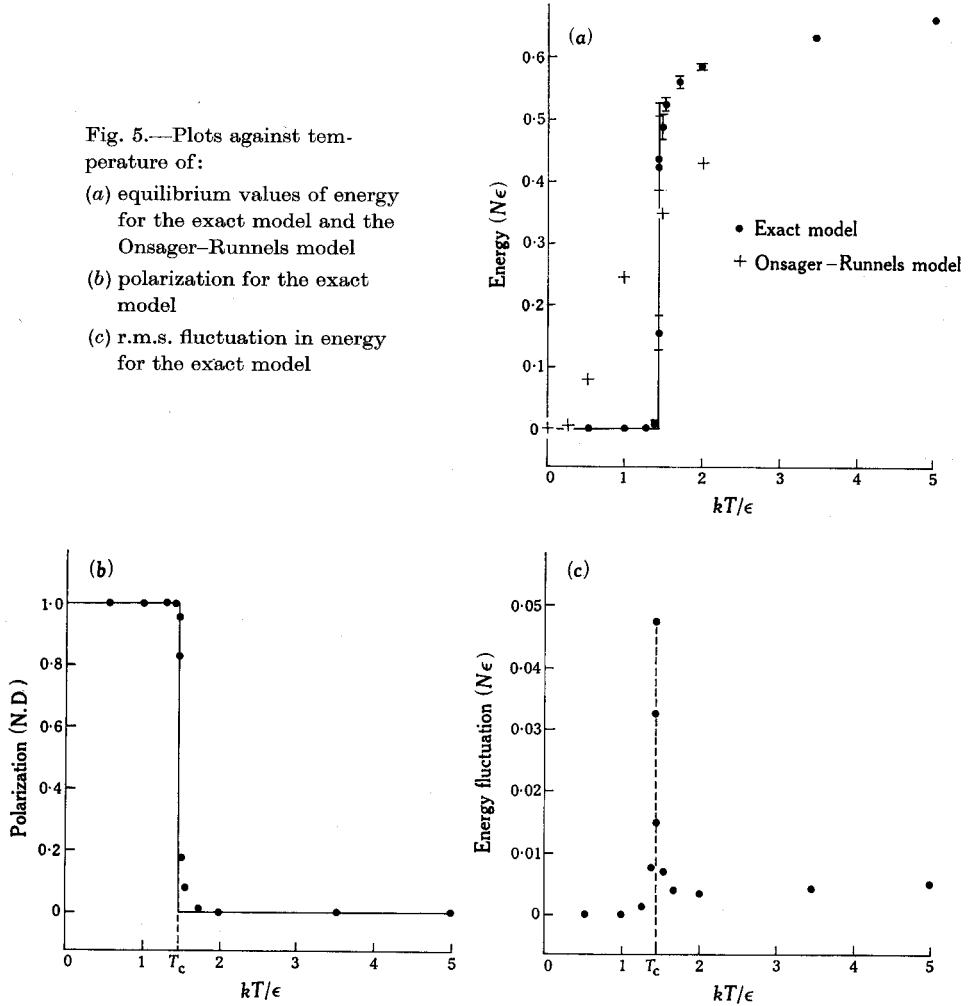
VI. RESULTS

(a) *Equilibrium Behaviour*

Computer runs were done at various temperatures ranging from $kT/\epsilon = 0.5$ to 10.0 , concentrating near the critical point at $kT_c/\epsilon = (\ln 2)^{-1} = 1.44265 \dots$. The equilibrium values of energy and polarization as a function of temperature are shown in Figures 5(a) and 5(b). The solid curve is the solution given by Lieb (1967a, 1967b, 1967c, 1967d). Points are plotted for the simulation of both the exact Slater-Onsager

model and the Onsager–Runnels approximation. The error bars represent the accuracy with which the mean value was determined, and not the fluctuation size. The errors in the mean values of the exact model are due to the long runs necessary to reach equilibrium and the large fluctuations that necessitated extremely long runs to achieve any sort of accuracy. The extent of the fluctuations of the exact model

Fig. 5.—Plots against temperature of:
 (a) equilibrium values of energy for the exact model and the Onsager–Runnels model
 (b) polarization for the exact model
 (c) r.m.s. fluctuation in energy for the exact model



is shown in Figure 5(c). It can be seen that the exact model fits Lieb's solution extremely well throughout the range. The half-width of the transition point is $\Delta T/T_c \sim 1 \times 10^{-2}$, which is reasonably sharp considering the number of lattice points is 10^4 . This close fit to Lieb's static solution confirms the validity of our model, and our computer simulation.

In fact, we can calculate the expected width of the transition region for a finite system. Using simple statistical mechanics, we have $\Delta E/E = f^{-\frac{1}{2}}$, where f is

the number of degrees of freedom and is of the order of 10^4 . Hence

$$\Delta E/E = 10^{-2}.$$

We also have

$$\partial E/\partial T = E^2/kT^2f,$$

and hence

$$\Delta T/T = (\Delta E/E)(fkT/E).$$

Near (and above) the critical temperature, kT/E is of order 10^{-4} . Hence $\Delta T/T = 10^{-2}$ and the width of the critical region in the computer simulation is comparable with the expected temperature resolution of the finite lattice.

Since $\Delta T/T = f^{-1/2} \sim N^{-1/2}$, where N is the number of lattice points, to achieve an accuracy one order better than these results we would need $N = 10^6$. Thus, using a 128×128 lattice ($N = 16384$) could not be expected to give appreciably better results. In fact, the present results with a 128×128 lattice were not noticeably different from the results with a 100×100 lattice. To use a 1000×1000 lattice ($N = 10^6$) would use more storage than exists in available computers, and would take many hours to reach equilibrium even with the fastest available computer.

The Onsager-Runnels approximation, on the other hand, gives very different results. There is no transition point at any temperature, both energy and polarization varying continuously. The high temperature limit of energy and polarization is the same as the exact solution.

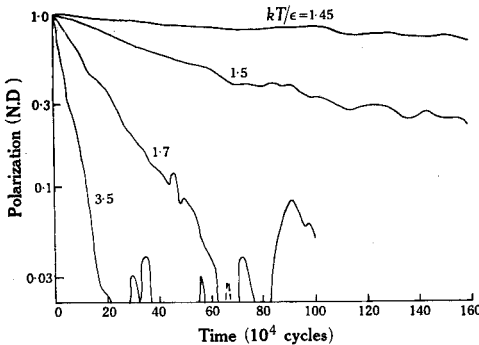


Fig. 6.—Time variation of polarization at various temperatures.

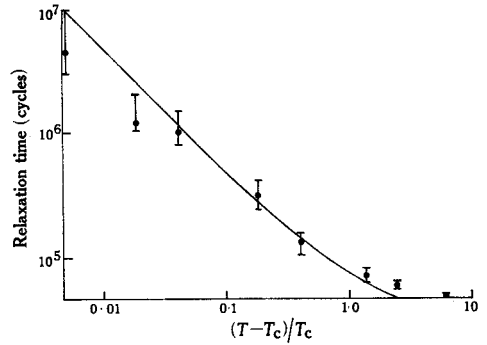


Fig. 7.—Log-log plot of relaxation time against $(T - T_c)/T_c$.

(b) Relaxation Phenomena

Figure 6 shows the time variation of polarization when the lattice is released from its ground state (i.e. zero temperature) and allowed to come to equilibrium at various temperatures. It can be seen that for all temperatures above the critical temperature, the polarization decays exponentially towards zero, until the equilibrium fluctuations in the polarization start to become dominant. The extent of the equilibrium fluctuations is shown in Figure 5(c).

Figure 7 shows a log-log plot of the relaxation time of polarization versus $(T - T_c)/T_c$. This is approximately a straight line with a gradient of about $-\frac{2}{3}$.

Changes in relaxation times of more than two orders of magnitude, over the range of temperatures from $kT/\epsilon = 10$ to 1.443 were obtained, dramatically demonstrating the critical slowing down of the model. The exponent $-\frac{2}{3}$ was smaller in magnitude than the result $(-\frac{7}{4})$ of Ogita *et al.* (1969) for the 2D Ising model.

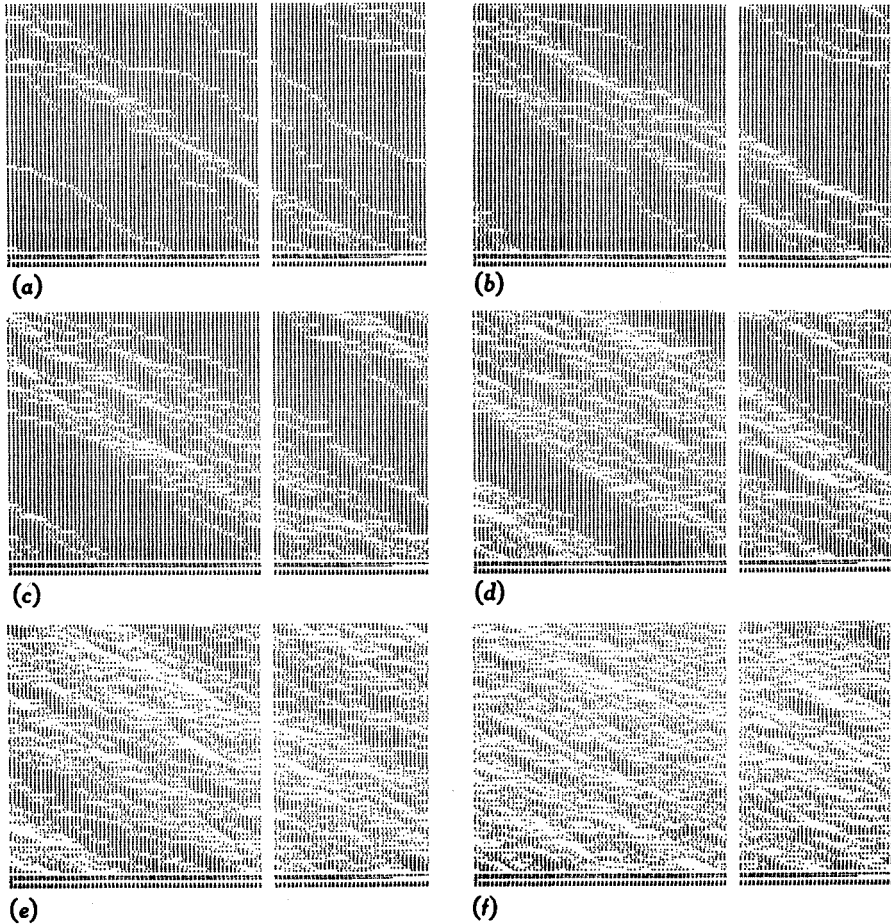


Fig. 8.—Examples of patterns showing polarization of the whole system for $kT/\epsilon = 1.470$ after various time intervals:

- (a) after 6×10^5 cycles, (b) after 1.2×10^6 cycles, (c) after 2×10^6 cycles,
 (d) after 4×10^6 cycles, (e) after 8×10^6 cycles, (f) at equilibrium.

The dots represent positive polarization and the blank areas, negative polarization.

A very clear understanding of the microscopic mechanism responsible for the critical slowing-down phenomenon can be had by studying the bond configurations of the lattice as it proceeds towards equilibrium. A typical series of such diagrams is shown in Figure 8. Here the dots represent positive polarization and the blank areas, negative polarization. By studying series of these diagrams at various temperatures, it could be seen that, at high temperatures, defects propagated reasonably efficiently

through the ground state lattice. As the temperature approached the critical temperature, the defect propagating in the ground state lattice became more and more likely to jump one step back, "unflipping" a bond it had previously "flipped". The probability of unflipping a previously flipped bond became equal to the probability of flipping a new bond at the critical temperature. Thus the mean velocity of the defect through the ground state lattice became zero at $T = T_c$. For $T < T_c$, the mean velocity was negative and defects always retraced their paths to annihilate with their antidefects. For $T > T_c$, the mean velocity was positive in the ground state and defects propagated freely until the lattice was in a totally disordered state. In fact, the mean velocity of propagation varies continuously and smoothly with temperature. The relaxation time, which one expects to be proportional to the inverse of the mean velocity, has a singularity at $T = T_c$. Since the temperature gradient of the mean velocity is finite for $T = T_c$, we expect the relaxation time to vary as $\{(T - T_c)/T_c\}^{-1}$ near the critical point. The variation of mean velocity with temperature in the ground state is shown in Figure 9, and the relaxation times derived from this curve are shown as a solid line in Figure 7.

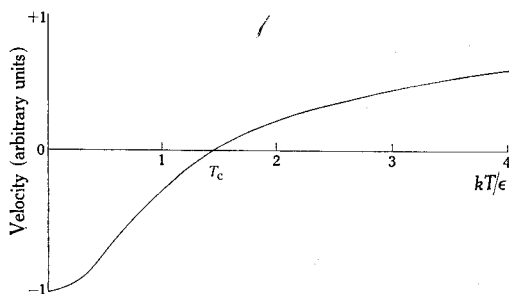


Fig. 9.—Variation of the mean velocity of defect propagation plotted against temperature in the ground state. The relaxation times derived from this curve are shown as a solid line in Figure 7.

The Onsager–Runnels approximation had no anomalous dynamic behaviour. The propagation of defects in the ground state lattice occurred with a positive, nonzero, mean velocity at all temperatures, giving this model all the characteristics of the exact model in the limit of high temperatures.

VII. DISCUSSION

The present dynamical model of the Slater K.D.P. model gives excellent agreement with the static exact solution of Lieb, as well as giving an insight into the nature of the critical transition. The computer simulation demonstrates the relationship between microscopic behaviour and the macroscopic results, particularly in showing the way small smooth microscopic changes can lead to the large discontinuous changes associated with critical phenomena. Although the formalism of the exact macroscopic system is formidable, approximations introduced to simplify the macroscopic system change the microscopic behaviour and destroy the nature of the transition.

Although the model was adapted to include an external electric field and results were obtained, they are not included here, as the external field does not play any great role in the critical phenomena and does not contribute to the clarification of the nature of the transition.

VIII. ACKNOWLEDGMENT

I wish to thank Professor C. A. Hurst for his discussions and assistance during the course of this work.

IX. REFERENCES

- BJERRUM, N. (1951).—*Biol. Skr.* **27**, 1.
GLAUBER, R. J. (1963).—*J. math. Phys.* **4**, 294.
KAWASAKI, K., and YAMADA, T. (1967).—*Phys. Lett. A* **25**, 192.
LIEB, E. H. (1967*a*).—*Phys. Rev. Lett.* **18**, 692.
LIEB, E. H. (1967*b*).—*Phys. Rev. Lett.* **18**, 1046.
LIEB, E. H. (1967*c*).—*Phys. Rev. Lett.* **19**, 108.
LIEB, E. H. (1967*d*).—*Phys. Rev.* **162**, 162.
OGITA, N., UEDA, A., MATSUBARA, T., MATSUDA, H., and YONEZAWA, F. (1969).—*J. phys. Soc. Japan (Suppl.)* **26**, 145.
ONSAGER, L. (1944).—*Phys. Rev.* **65**, 117.
ONSAGER, L., and DUPUIS, M. (1960).—*Supplto nuovo Cim.* **10**, 294.
ONSAGER, L., and DUPUIS, M. (1962).—“Electrolytes.” pp. 27–46. (Pergamon Press: Oxford.)
SLATER, J. C. (1941).—*J. chem. Phys.* **9**, 16.

